Assesment of β-lapachone loaded in lecithin-chitosan nanoparticles for the topical treatment of cutaneous leishmaniasis in *L. major* infected BALB/c mice

Esther Moreno[a,b,1], PhD, Juana Schwartz[a,c,1], Esther Larrea[a,b], PhD, Iosune Conde[c], Maria Font[a,b,d], PhD, Carmen Sanmartín[a,b,d], PhD, Juan Manuel Irache[b,c], PhD and Socorro Espuelas[a,b,c,*], PhD

[a] Institute of Tropical Health, University of Navarra, [b] Instituto de Investigación Sanitaria de Navarra (IdISNA), [c] Pharmacy and Pharmaceutical Technology Department, University of Navarra and [d] Organic and Pharmaceutical Chemistry Department, University of Navarra, 31008 Pamplona, Spain

* Corresponding author address: Institute of Tropical Health, Pharmacy and Pharmaceutical Technology Department, IdISNA, University of Navarra, 31008 Pamplona, Spain.
Tel.: +34 948425600; Fax: +34 948425649. E-mail address: sespuelas@unav.es

1 The authors have contributed equally to this work.

Abstract

Patients affected by cutaneous leishmaniasis need a topical treatment which cures lesions without leaving scars. Lesions are produced not only by the parasite but also by an uncontrolled and persistent inflammatory immune response. In this study, we proposed the loading of β-lapachone (β-LP) in lecithin-chitosan nanoparticles (NP) for targeting the drug to the dermis, where infected macrophages reside, and promote wound healing. The loading of β-LP in lecithin-chitosan NP was critical to achieve important drug accumulation in the dermis and permeation through the skin. In addition, it did not influence the drug antileishmanial activity. When topically applied in *L. major* infected BALB/c mice,

1

β-LP NP achieved no parasite reduction but they stopped the lesion progression. Immuno-histopatological assays in CL lesions and quantitative mRNA studies in draining lymph nodes confirmed that β-LP exhibited anti-inflammatory activity leading to the downregulation of IL-1β and COX-2 expression and a decrease of neutrophils infiltrate.

Background

Currently, cutaneous leishmaniasis (CL) is considered as a major global health problem. Over 12 million people suffer from this neglected disease worldwide and, approximately, 1.5 million people are infected annually. CL shows different clinical manifestations depending on the *Leishmania* specie implicated in the infection. Some forms of the disease can exhibit localised ulcerative skin lesions (LCL) that may spontaneously heal while other forms can diffuse (DCL) or lead to significant mucosal tissue destruction and disfigurement (MCL) [1]. In general, species that are prevalent in the Old World (OWCL) produce limited clinical manifestations compared with New World species (NWCL) [2].

Presently, there is no satisfactory therapy for CL. The World Health Organization (WHO) recommends the topical treatment for uncomplicated LCL, although if the topical treatment fails or the patient has a more severe forms of the disease, the experts advice the parenteral therapy [1, 3]. Topical treatments present advantages such as better patient compliance and lower systemic toxicity and costs [4]. Among the topical treatments, paramomycin (PM) has been used in several formulations for more than 40 years. In spite of the variable cure rate that some studies showed (from 9% to 90% against OWCL and NWCL species) [2], a meta-analysis of 14 randomised controlled trials confirmed that topical PM was as effective as intralesional antimonials in treating OWCL and less effective against NWCL. Besides, the ointment produced skin irritation [5]. Thus, recent clinical trials confirmed the effectiveness and well-tolerance of the PM-based formulation WR279396, which contained 15% PM and 0.5% gentamicin, in ulcerative CL lesions produced by *L. major* [6] and *L. panamensis* [7]. However, further studies are necessary regarding to drug development, delivery, safety, efficacy and costs.

New topical products for CL treatment are expected to accelerate parasite clearance, prevent parasite dissemination and reduce the chance of relapse. Furthermore, they should exhibit more rapid and stable repair processes that do not lead to scars and disfigurement [4]. These properties rely on the ability of the formulation to deliver the active compound in the infected macrophages residing in the dermis in amount and time enough to destroy parasites and modulate the immune response in a manner that contributes to eradicate the parasite avoiding ulcer formation and tissue destruction [8].

β-lapachone (β-LP), a *o*-naphthoquinone obtained from the bark of the Lapacho tree (*Bignoniaceae* family, *Tabebuia* sp.) exhibits a wide range of activities including antitumor, antifungal, antiviral, antibacterial or antitrypanosomal properties [9]. Furthermore, its antileishmanial activity has been

tested *in vitro* against *L. infantum* and *L. amazonensis* with a $IC_{50} < 3$ μM [10]. β-LP has intrinsic antileishmanial activity and physicochemical characteristics that could be of interested to permeate and penetrate through the skin such as low molecular weight (242.3 Da) and suitable log *P* (2.5). Besides, *in vitro* and *in vivo* studies have demonstrated the efficacy of β-LP in promoting wound healing [11, 12]. Because of these reasons, we decided to evaluate this drug formulated in lecithin (LEC)-chitosan nanoparticles (NP) for the topical treatment of CL. Nanocarriers such as polymeric particles, microemulsions, liposomes or lipidic NP have demonstrated the ability to increase drug solubility and enhance the penetration and permeation of drugs into and through the skin. They also offer better controlled release properties than the classical topical formulations such as hydrogels, ointments or creams, due to the fact that they prevent rapid clearance to systemic circulation and systemic side effects [13, 14]. Formulations based on LEC-chitosan NP have been reported as topical delivery systems for drugs. Active agents such as clobetasol-17-propionate [15], quercetin [16] or diflucortolone [17] that have been loaded in LEC-chitosan NP have enhanced their permeation ability and increased their skin accumulation compared with creams or gels.

With this purpose, in the present study, LEC-chitosan NP loaded with β-LP were prepared and evaluated *in vitro* against *L. major* parasites and peritoneal macrophages. Moreover, studies to examine the capacity of the formulations to permeate and penetrate across pig ear skin as well as their effect on wound healing were carried out. Finally, their efficacy was determined for the topical treatment of CL lesions in *L. major* infected BALB/c mice.

Methods

Preparation and characterization of β-lapachone nanoparticles

β-LP NP were prepared following the procedure reported by Sonvico et al. with modifications [18]. Briefly, chitosan (Q 95/100, 1% w/v) was solubilized in 2% w/v lactic acid and β-LP (10 mg/mL) was also dissolved in an ethanolic solution of LEC. The organic phase was prepared by mixing LEC:DDAB solutions (60:30 mM, respectively) or LEC:MNL solutions (75:45 mM, respectively) in ethanol: acetone (5:4 v/v). Afterwards, β-LP NP suspensions were obtained by injection of 4 mL of this organic mixture into 4 mL of the chitosan solution. The organic solvents were evaporated and the non-entrapped β-LP was separated by centrifugation. The β-LP NP were recovered for further characterization and the encapsulation efficiency was determined by UV-Visible spectrophotometry.

In vitro permeation studies

Permeation studies using Franz diffusion cells were carried out in pig ear skin according to OECD guideline 428. The amount of β-LP in the skin samples was quantified by HPLC-UV.

Effect of β-lapachone and β-lapachone nanoparticles on L. major amastigotes in vitro

Macrophages were infected with metacyclic promastigotes of *L. major* (clone VI, MHOM/IL/80/Friendlin) in a 7:1 proportion (parasites:macrophages). Infected cells were treated with β-LP, β-LP NP or unloaded NP with or w/o Imiquimod (IMQ, 0.1 µg/mL). After 48 hours, slides were fixed and stained for evaluation [19]. The percentage of infected macrophages was evaluated by counting 200 macrophages using an optical microscope. Nitric oxide (NO) in cell culture supernatants was determined by the Griess reaction.

In vivo evaluation of β-lapachone formulations in L. major-infected BALB/c mice

The infected mice were randomly separated in cages (5 animals per cage) and two different treatments were evaluated and compared with non-treatment infected mice (control). The groups were: 20 mg/kg of β-LP NP and the equivalent of unloaded NP applied topically. Lesions were covered with 100 µL of the NP formulations (β-LP NP (5 mg/mL) or unloaded NP). Topical treatment was applied daily for a period of 21 days.

Histological analysis and immunohistochemistry

Skin sections were stained with hematoxylin and eosin (H&E) and Masson trichrome. Immunohistochemistry was applied using the following primary antibodies: rat anti-mouse F4/80 (1:400; eBiosciences, 14-4801), rat anti-mouse NIMP-R14 (1:10000; Abcam, ab2557), rabbit anti-CD3 (1:300; Thermo Scientific, RM9106) and rabbit anti-iNOS (1:500; Santa Cruz Biotechnology, sc-650). Then, the EnVision system (Dako, K4011) was used in all cases according to manufacturer instructions. For each assay, digital images were obtained and the area percentage stained in each image was quantified using Fiji 2.0 software.

RNA extraction and quantitative real time RT-PCR

IL-1β, Cox-2, iNOS, IL-4, TNF-α, IFN-γ, TGF-β and β-actin expression were measured in the mice skin lesions and draining lymph nodes by quantitative real time PCR using iQ SYBR Green supermix (Bio-

Rad) and specific primers for each gene (see Supplementary Table 1) in a CFX96 system from Bio-Rad.

The *in vitro* antileishmanial activity against *L. major* promastigotes, *in vitro* cytotoxicity assay in mouse peritoneal macrophages, wound healing studies, statistical analysis and further details of the experiments can be found in the Supplementary Materials

Results

Preparation and characterization of β-lapachone nanoparticles

LEC-chitosan NP containing MNL or DDAB were prepared and, particle size (Ø), polydispersity index (PDI), Z-potential and encapsulation efficiency (EE) were determined in order to characterise the NP (Table 1). The mean size of the NP prepared for this study ranged from 317 to 574 nm, showing LEC:DDAB NP smaller sizes than LEC:MNL NP. The Z-potential value was higher for the NP containing DDAB (around 90 mV) than those containing MNL (around 30 mV) but in all cases they were positively charged. Moreover, NP suspensions were found to have a suitable PDI, ranging from 0.21 to 0.27. Compared to LEC:MNL NP, LEC:DDAB NP were observed to have better EE and exhibited 2-fold higher β-LP loadings (25.8 and 52.4, respectively).

In vitro skin permeation studies

To assess the influence of the LEC-chitosan NP on the permeation and accumulation of β-LP into the skin, *in vitro* skin studies were performed in pig ear skin using Franz diffusion cells. In this study, the two chitosan-NP formulations, LEC:DDAB NP and LEC:MNL NP, were also compared with a β-LP chitosan hydrogel. It was observed that the β-LP hydrogel cession capacity was the lowest among the different skin layers and the receptor compartment (RC) in the three skin models (intact skin, tape stripped and dermal membranes, Figure 1A-C). This cession capacity increased when dermal membranes were used, rising from 0.24 to 1.25% the total percentage of β-LP in the hydrogel. As it was expected, the total amount of β-LP quantified in the LEC:DDAB NP was higher in the ulcerative skin models than in intact skin (1.67, 4.47 and 16.10% for intact skin, tape stripped and dermal membranes, respectively). Although the total amount of β-LP found in intact skin was similar if we compare LEC:DAAB NP with LEC:MNL NP (Figure 1A), it is important to point out that the amount of

drug determined in the 900 μm thick skin layer (that simulates the dermis) was 10-fold higher in the case of LEC:DDAB NP (0.09 and 0.95%, respectively). Finally, in the three skin models the incorporation of the β-LP into LEC:DDAB NP notably enhanced the retention of the drug in the dermis (900 μm) compared with the other formulations.

In vitro antileishmanial activity and cytotoxicity studies

The antileishmanial activity assay in *L. major* promastigotes treated with β-LP and β-LP loaded NP revealed that the encapsulation of the drug into the two NP formulations did not affect its leishmanicidal activity (Table 2) because they have comparable IC_{50} values (IC_{50} = 2.6 μM for LEC:MNL NP and IC_{50} = 1.9 μM for LEC:DAAB NP). Besides, cytotoxicity studies in peritoneal macrophages showed that when β-LP was incorporated into the NP, the toxicity increased moderately (IC_{50} = 2.1 μM for LEC:MNL NP and IC_{50} = 3.4 μM for LEC:DAAB NP compared with a IC_{50} = 6.3 μM for free β-LP). As the LEC-chitosan NP prepared with MNL or DDAB had similar promastigotes activity and toxicity, the activity in intracellular amastigotes was only performed with LEC:DDAB NP due to their higher EE and higher permeation and penetration values through the skin. As it is shown in Table 3, a 2-fold higher antileishmanial activity of free β-LP in the amastigote form compared with the promastigote form can be clearly stated (IC_{50}= 0.7 and IC_{50}= 1.5, respectively). Moreover, β-LP loaded NP, prepared with DDAB, presented higher activity in the amastigote form (IC_{50}= 0.3), being 6 times more potent in the amastigote form than in promastigotes (IC_{50}= 1.9), which suggests a possible immunomodulatory effect for the system. Furthermore, β-LP NP showed less toxicity than free β-LP because it presents a selectivity index (SI) value of 11.3 instead of 9.1. A dose-response effect could also be observed when increasing concentrations of β-LP or β-LP NP were used (Figure 2A). This led to a decrease from 46 to 11 in the number of amastigotes per 100 macrophages ($p < 0.05$) at 1 μM concentration (compared to control). The combination of β-LP NP with the immunomodulator IMQ also produced a significant decrease at 1 μM ($p < 0.05$) although an increase in the number of amastigotes was observed at low concentrations (0.01 and 0.1 μM) when β-LP was combined with IMQ (Figure 2B). In the case of unloaded NP, concentrations of these NP alone or in combination with IMQ reduced *L. major* infection (Figure 2C). This reduction was significant at 1 and 10 μM of unloaded NP and also at 10 and 20 μM of unloaded NP with IMQ ($p < 0.05$). Moreover, unloaded NP at 20 μM caused a very significant decrease in the number of amastigotes ($p < 0.01$). Regarding the NO concentration determined in the supernatants of infected macrophages, there were no remarkable

changes in the production of NO by infected macrophages after treatment with β-LP or β-LP NP alone or combined with IMQ (Figures 2D and 2E). However, an increase in the production of NO was observed after 48 hours treatment with unloaded NP alone or with IMQ at 1, 10 and 20 µM (Figure 2F). The highest NO production corresponded to 20 µM of unloaded NP combined with IMQ, in which NO production increased from 4 µM in control cells to 27 µM. These results suggest that, at higher concentrations, the system could have an effect in the activation of macrophages, leading to NO production.

Wound healing studies

Previous studies showed the activity of β-LP in accelerating wound healing [11, 12]. Cytotoxicity studies after 24 hours revealed that after treatment with β-LP at 1 and 2.5 µM a slightly increase in cell proliferation was observed (Supplementary Figure 1A). It was also observed that with the highest concentrations of unloaded NP (100, 250 and 500 µM) cell proliferation increased in a dose-dependent manner (Supplementary Figure 1B). Moreover, neither the β-LP nor the NP improved the healing percentage in 3T3 fibroblasts after 12 hours (Supplementary Figure 1C).

Efficacy of β-lapachone NP in L. major infected BALB/c mice

To evaluate the *in vivo* efficacy of β-LP NP in the treatment of CL lesions, BALB/c mice were infected subcutaneously by inoculating 2×10^5 metacyclic promastigotes of *L. major* in the base of the tail. The infection induced a progressive increase in the lesion size in all the animals and no statistical significant differences were observed between mice before treatment ($p > 0.05$). After 5-7 weeks, treatments were started and, although a slightly reduction in size area was observed in mice treated with unloaded NP during the first 2 weeks, similar lesions to control group (untreated group) developed at the end of treatment (21 days). In contrast, treatment with β-LP NP resulted in a significant reduction in lesion size compared with the control group, from 61.2 ± 21.2 (control group) to 35.7 ± 29.4 ($p < 0.05$, topical β-LP NP) (Figure 3A and Figure 3B). Moreover, it can be seen in Figures 3C-F that topical treatment with unloaded or β-LP loaded NP did not lead to a reduction in the parasite burdens of skin, liver, spleen or draining lymph node compared to the control group.

Histopathology and immunohistochemistry of CL lesions

Histopathological and immunochemistry investigations were performed to evaluate the effect of the treatment and to confirm the macroscopic reduction of the lesion size. At the end of the experiment, control mice (untreated) showed CL lesions in which two different regions were observed: i) the ulcer focus, corresponding to the scab and necrotic and granulotic tissue (Supplementary Figure 2D) and ii) an area characterised by an epidermal hyperkeratosis and enormous inflammation that invaded subcutaneous and muscular tissues (Supplementary Figures 2B and 2C). Immunohistochemistry showed that the inflammatory infiltrate was mainly composed of macrophages (16%), neutrophils (39%), and also lymphocytes (2.1%). Whereas the neutrophils were mainly located in the necrotic region (Figures 4C and 4G), *L. major* infected macrophages and free parasites were the dominant cellular infiltrate within the non-necrotic and inflamed tissue in both untreated and treated mice (Figures 4D and 4H, supplementary Figures 2B and 2C). In the β-LP NP treated mice, we observed that the necrotic area, the depth of the inflammatory infiltrate that does not reach the muscular tissue (Figure 4E), as well as the neutrophils (Figures 4G and 4I), decreased.

Real time-PCR studies

The expression at the transcripcional levels of several cytokines (TNF-α, IL-1β, IL-4, TGF-β, IFN-γ) and markers (COX-2, iNOS) associated either with skin inflammation or CL lesion outcome were analysed in the CL lesions and draining lymph nodes. Results showed that there were no differences in skin IFN-γ, IL-4, TNF-α, iNOS or TGF-β between treated and non-treated mice (data not shown). Although the highest expression was seen in the lesion (data not shown), only significant differences between control and β-LP treated mice in IL-1β and COX-2 expression were detected in the draining lymph nodes (Figures 5A and 5B).

Discussion

Looking for a better CL topical therapy and aiming to explore the goodness of NP skin delivery in CL lesions, in the current study, β-LP was encapsulated in NP containing LEC, a safe and biocompatible excipient widely used in delivery systems, as well as chitosan, an antimicrobial agent with penetration-enhancing properties. Moreover, DDAB or MNL, two different lipids with antimicrobial activity [20, 21] and different charge, were also included into the formulations to investigate if they could affect either the β-LP skin delivery and/or the anti-leishmanial activity. Permeation and penetration studies

confirmed that β-LP loaded in LEC-chitosan NP containing DDAB presented a higher ability than NP containing MNL and chitosan hydrogel to penetrate and also to permeate across the intact skin or dermal membranes (Figure 1A and 1C). The ability of chitosan and LEC-chitosan NP to enhance skin penetration has been previously demonstrated with several drugs [15-17]: the positive charge of chitosan ensured close contact between the NP and the skin and produced an occlusive barrier that increased the hydration. This occlusion is known to facilitate the permeation of the drugs into the skin. Besides, DDAB could disrupt the lipid bilayers of skin and further facilitate the drug permeation [22].

Upon arrival in the dermis, the efficacy of the topical therapy will be determined by the activity of the formulation against intramacrophagic amastigotes. The results (Table 2) showed a high activity of β-LP against *L. major* parasites and a SI around 9 (Table 2), better than what had been previously described with *L. infantum* and *L. amazonensis* [10]. The encapsulation of the drug in the NP slightly modified the drug activity and the therapeutic index although unloaded vesicles also showed leishmanicidal effect against promastigotes (Table 2) and amastigotes (Table 3 and Figures 2A-C). We hypothesise that the positively charged NP may interact with the negatively charged parasites producing disruption of the membrane and the death of the parasite. The superior efficacy against intramacrophagic amastigotes (IC_{50} of 117.7 vs 3.5 against promastigotes and amastigotes, respectively) would indicate that unloaded NP produced macrophage-mediated leishmanicidal mechanisms. This immunostimulatory effect was confirmed by NO production, which closely correlated with the parasite elimination in a concentration-dependent manner (Figures 2C and 2D). The role of NO production by the inducible NO synthase (iNOS) in killing *L. major* parasites *in vitro* and for controlling the infection *in vivo* is well-known [23]. It has been previously described the ability of DDAB liposomes to generated reactive oxygen species (ROS) and activated p38 MAPK, implicated in iNOS expression through IL-12 or TNF-α production [24]. Furthermore, a recent work described the leishmanicidal effect of phosphatidylcholine DDAB liposomes against *L. donovani* promastigotes and amastigotes, being their activity superior to other cationic liposomal formulations [21]. Similarly, other cationic NP, chitosan-nanoemulsion templates, improved AmB leishmanicidal activity [25] and enhanced iNOS and TNF-α expression were determined in the hamster splenocytes

However, although NP induced NO production *per se* in the infected macrophages and the loading of β-LP in NP was addressed with the aim to both target the drug to macrophages and concurrently activate their microbial mechanisms, β-LP NP had similar antileishmanial activity than the free drug

(Figure 2A) and no significant NO production was observed (Figure 2D). A certain anti-inflammatory activity of β-LP has been previously described *in vitro* in LPS-stimulated alveolar and RAW 264.7 macrophages [26] and *in vivo* in LPS-induced lung edema [26]. β-LP inhibited NF-κB and ERK1/2 activation, down-regulating iNOS expression and TNF-α release [26]. Our results could indicate that the drug may also inhibit cationic NP-mediated macrophage activation and, consequently, the NO production (Figure 2D).

Because of the lack of immunostimulatory effect of β-LP NP, we decided to study β-LP and β-LP NP efficacy co-administered with the immunomodulator IMQ, a TLR7 agonist, known to activate NF-κB transcription factor and produce TNF-α and NO. IMQ is currently the only topical immunotherapeutic approach assayed in patients affected by CL with variable success [27]. It has been reported that IMQ administered alone at 1 μg/mL produced complete elimination of *L. donovani* intracellular amastigotes [28]. In fact, an interaction between PM and IMQ was previously described [29]. Aiming to find out if β-LP could lead to a higher activity with IMQ, 0.1 μg/mL IMQ were co-administered with β-LP, β-LP NP or unloaded NP in this work. However, no modifications of their activity (Figures 2A-C) were detected. In agreement with this, NO production by infected macrophages was similar with or without the IMQ co-administration (Figures 2D-F).

There are many antileishmanial drugs with immunomodulatory activities [30] whose loading in immunoadjuvant carriers or their co-administration with immunostimulants have been proposed as a mean to both enhance the drug targeting and the host immune response [21, 25, 31]. However, there are compounds that display dual immune effect depending on the immune environment. I.e. berberine [32] and 18b-glycyrrhetinic acid [33] had antileishmanial activity via MAPKinases, iNOS induction and NO up-regulation. However, they showed inhibitory effects on LPS-iNOS in macrophages [34, 35]. Thus, we should keep in mind that the loading of immuno-active drugs in NP could greatly affect their activity as well as the effect produced by the unloaded carriers.

The acceleration of the lesion healing should be another characteristic of topical CL therapy and this was one the reasons why β-LP was chosen as the drug candidate. Previous studies demonstrated that β-LP promoted the proliferation of keratinocytes, fibroblasts and endothelial cells, the migration of fibroblasts and endothelial cells, induced macrophages to release VEGF and EGF and thus accelerate wound healing in C57BL/6 mice [11, 12]. On the other hand, several studies support the use of chitosan to treat wound infections [36] by mechanisms such as reduction of TNF-α mRNA expression

and induction of VEGF production by macrophages [37]. In the current study, although β-LP (1-2.5 µM) and unloaded NP (> 100 µM DDAB) induced 3T3 fibroblast proliferation (Supplementary Figure 1A and 1B), no effect was observed in the healing of scratches in fibroblast monolayers (Supplementary Figure 1C). The effects of chitosan in macrophages and fibroblasts can be highly affected by factors such as the molecular weight and the deacetylation degree (DDA) [36] [38]. In the current study, we used a chitosan with high molecular weight and high DDA (Q 95/100) and this type of chitosans have been previously reported as stronger activators than small chitosans or their oligomers. Currently, it is not known whether their formulation in NP could affect the process of wound healing.

Based on the good intrinsic antileishmanial activity of β-LP and the enhancement in β-LP skin penetration mediated by LEC-chitosan-DDAB NP delivery, we addressed the *in vivo* evaluation of the formulation efficacy in *L. major* infected BALB/c mice. The topical and daily application of β-LP NP did not clear the infection but delayed the lesion progression. Unlike humans, where ulcerative CL are associated with low infectious loads and non-ulcerative lesions with impaired parasite clearance, the BALB/c murine CL model is always associated with widespread tissue destruction and uncontrolled parasite replication provoked by persistence of Th2 cells and IL-10, resulting in chronic tissue remodelling with necrosis and fibrosis. Thus, in BALB/c mice the size of the lesion may reflect the parasite burden as well as the degree of inflammation caused by the host immune response to the parasite [39]. In our work, the immunohistopatology of the lesions showed that, after the treatment, the tissue surrounding the ulcers, which presented epidermal hyperkeratosis, and massive infiltration of infected macrophages were similar (Figures 4A and 4E). However, β-LP decreased the ulceration area, crust and necrosis with infiltrated neutrophils (Figure 4E). This effect was associated with a significant reduction in the mRNA expression of IL-1β and COX-2 (Figures 5A and 5B). β-LP was previously described to attenuate the expression of IL-1β and COX-2 *in vitro* in LPS-stimulated BV2 microglia [40]. Elevated levels of IL-1β and IL-1 mediated inflammosome family proteins are implicated in chronic and non-healing wounds of diabetic mice and in several autoinflammatory diseases characterized by recurrent episodes of skin lesions [41]. Mice with hyperactive inflammosome developed a neutrophil rich inflammation of skin [42] and the persistence of neutrophils in the wound is associated with delayed healing, excessive scar formation and significant tissue damage to the host [43]. Therefore, IL-1 induced COX-2 expression and the synthesis of PEG2, well-known lipid mediator

of manifestations of skin inflammation such as edema and increased vascular permeability with influx influx of neutrophils and macrophages [44] .

On the other hand, studies about the effect of IL-1β in the parasite were only made early after parasite infection giving contradictory results depending on the *Leishmania* species. Whereas it contributed to NO-mediated resistance to *L. amazonensis*, *L. braziliensis and L. infantum-chagasi* [45], IL-1 production was irrelevant [46] or detrimental in early *L. major* infections and the effect should be mediated by Th2-bias adaptive immune response [47]. IL-1b was one of the genes significantly stronger up-regulated in resistant C57BL/6 mice vs susceptible BALB/c mice although the analysis was made from 16 h *L. major* infected mice [48]. Our study would indicate poor contribution of IL-1b in the chronic state of the infection.

COX-2 mediated PGE2 production is a mechanism for which *Leishmania* parasite suppressed macrophage activation and COX-2 inhibition could thus favour the elimination of *Leishmania* parasites. However, COX-2 expression was high in self-controlled lesions of C57BL/6 mice and in severe lesions in BALB/C mice infected with *L. amazonensis*. Moreover, its expression was not modified in BALB/c mice treated with antimonials [49]; the antileishmanial activity of glycyrrhizic acid was mediated by inhibition of COX-2 in *L. donovani* infected macrophages although, in that case, it was concomitant with enhanced expression of iNOS, IL-12, TNF-α and down-regulation of IL-10 and TGF-β [50]. In our study, β-LP COX-2 downregulation occurred without any modification of iNOS expression.

Finally, the effect of the neutrophils in *Leishmania* infection progression has been analysed only at the early onset of infection [51]. In *L. major* infected BALB/c mice, the early uptake of *Leishmania* infected neutrophils by macrophages exacerbated the infection by PEG2 and TGF-β production [52]. The pattern of exclusive distribution observed in our study (neutrophils in the necrotic area and macrophages in the inflamed tissue, Figures 4C and 4G vs 4D and 4H) when the infection is already well-established suggests that, at this time, neutrophils could influence the lesion progression but not the parasitic load evolution.

Overall, our data would indicate that topical β-LP NP treatment mediated the down-regulation of IL-1β and COX-2. This had no effect in the parasite elimination although the neutrophils infiltrate and tissue necrosis at the site of infection decreased. The role of epidermal cells such as keratinocytes and neutrophils has only been previously evaluated in early infected animals. However, the analysis of

their influence once *Leishmania* infection has been well-established could open new therapeutic strategies in the topical treatment of CL.

Acknowledgements

Bibliography

1   WHO, Control of the leishmaniasis: report of a meeting of the WHO Expert Committee on the Control of Leishmaniasis, Geneva, 22-26 March 2010. *WHO technical report series 949*. 1-185 **(2010)**

2   R. Reithinger, J. C. Dujardin, H. Louzir, C. Pirmez, B. Alexander, and S. Brooker, Cutaneous leishmaniasis. *Lancet Infect Dis*. 7, 581-96 **(2007)**

3   B. Monge-Maillo, and R. Lopez-Velez, Therapeutic options for old world cutaneous leishmaniasis and new world cutaneous and mucocutaneous leishmaniasis. *Drugs*. 73, 1889-920 **(2013)**

4   C. V. David, and N. Craft, Cutaneous and mucocutaneous leishmaniasis. *Dermatol Ther*. 22, 491-502 **(2009)**

5   D. H. Kim, H. J. Chung, J. Bleys, and R. F. Ghohestani, Is paromomycin an effective and safe treatment against cutaneous leishmaniasis? A meta-analysis of 14 randomized controlled trials. *PLoS Negl Trop Dis*. 3, e381 **(2009)**

6   A. Ben Salah, N. Ben Messaoud, E. Guedri, A. Zaatour, N. Ben Alaya, J. Bettaieb, A. Gharbi, N. Belhadj Hamida, A. Boukthir, S. Chlif, K. Abdelhamid, Z. El Ahmadi, H. Louzir, M. Mokni, G. Morizot, P. Buffet, P. L. Smith, K. M. Kopydlowski, M. Kreishman-Deitrick, K. S. Smith, C. J. Nielsen, D. R. Ullman, J. A. Norwood, G. D. Thorne, W. F. McCarthy, R. C. Adams, R. M. Rice, D. Tang, J. Berman, J. Ransom, A. J. Magill, and M. Grogl, Topical paromomycin with or without gentamicin for cutaneous leishmaniasis. *N Engl J Med*. 368, 524-32 **(2013)**

7   N. Sosa, Z. Capitan, J. Nieto, M. Nieto, J. Calzada, H. Paz, C. Spadafora, M. Kreishman-Deitrick, K. Kopydlowski, D. Ullman, W. F. McCarthy, J. Ransom, J. Berman, C. Scott, and M. Grogl, Randomized, double-blinded, phase 2 trial of WR 279,396 (paromomycin and gentamicin) for cutaneous leishmaniasis in Panama. *Am J Trop Med Hyg*. 89, 557-63 **(2013)**

8   E. Moreno, J. Schwartz, C. Fernandez, C. Sanmartin, P. Nguewa, J. M. Irache, and S. Espuelas, Nanoparticles as multifunctional devices for the topical treatment of cutaneous leishmaniasis. *Expert Opin Drug Deliv*. 11, 579-97 **(2014)**

9   E. de Almeida, Preclinical and clinical studies of Lapachol and Beta-lapachone. *The Open Natural Products Journal*. 2, 42-47 **(2009)**

10   T. T. Guimaraes, C. Pinto Mdo, J. S. Lanza, M. N. Melo, R. L. do Monte-Neto, I. M. de Melo, E. B. Diogo, V. F. Ferreira, C. A. Camara, W. O. Valenca, R. N. de Oliveira, F. Frezard, and E. N. da Silva, Jr., Potent naphthoquinones against antimony-sensitive and -resistant Leishmania parasites: synthesis of novel alpha- and nor-alpha-lapachone-based 1,2,3-triazoles by copper-catalyzed azide-alkyne cycloaddition. *Eur J Med Chem*. 63, 523-30 **(2013)**

11   S.-C. Fu, Y.-P. Chau, K.-S. Lu, and H.-N. Kung, beta-Lapachone accelerates the recovery of burn-wound skin. *Histology and Histopathology*. 26, 905-914 **(2011)**

12   H.-N. Kung, M.-J. Yang, C.-F. Chang, Y.-P. Chau, and K.-S. Lu, In vitro and in vivo wound healing-promoting activities of beta-lapachone. *American Journal of Physiology-Cell Physiology*. 295, C931-C943 **(2008)**

13   V. Dubey, D. Mishra, M. Nahar, and N. K. Jain, Vesicles as tools for the modulation of skin permeability. *Expert Opin Drug Deliv*. 4, 579-93 **(2007)**

14   M. Gupta, U. Agrawal, and S. P. Vyas, Nanocarrier-based topical drug delivery for the treatment of skin diseases. *Expert Opin Drug Deliv*. 9, 783-804 **(2012)**

15   T. Senyigit, F. Sonvico, S. Barbieri, O. Ozer, P. Santi, and P. Colombo, Lecithin/chitosan nanoparticles of clobetasol-17-propionate capable of accumulation in pig skin. *J Control Release*. 142, 368-73 **(2010)**

16   Q. Tan, W. Liu, C. Guo, and G. Zhai, Preparation and evaluation of quercetin-loaded lecithin-chitosan nanoparticles for topical delivery. *Int J Nanomedicine*. 6, 1621-30 **(2011)**

17   I. Ozcan, E. Azizoglu, T. Senyigit, M. Ozyazici, and O. Ozer, Enhanced dermal delivery of diflucortolone valerate using lecithin/chitosan nanoparticles: in-vitro and in-vivo evaluations. *Int J Nanomedicine*. 8, 461-75 **(2013)**

18   F. Sonvico, A. Cagnani, A. Rossi, S. Motta, M. T. Di Bari, F. Cavatorta, M. J. Alonso, A. Deriu, and P. Colombo, Formation of self-organized nanoparticles by lecithin/chitosan ionic interaction. *International Journal of Pharmaceutics*. 324, 67-73 **(2006)**

19   J. Giaimis, Y. Lombard, M. Makaya-Kumba, P. Fonteneau, and P. Poindron, A new and simple method for studying the binding and ingestion steps in the phagocytosis of yeasts. *J Immunol Methods*. 154, 185-93 **(1992)**

20   P. M. Schlievert, and M. L. Peterson, Glycerol monolaurate antibacterial activity in broth and biofilm cultures. *PLoS One*. 7, e40350 **(2012)**

21   R. Sinha, J. Roychoudhury, P. Palit, and N. Ali, Cationic Liposomal Sodium Stibogluconate (SSG), a Potent Therapeutic Tool for Treatment of Infection by SSG-Sensitive and -Resistant Leishmania donovani. *Antimicrob Agents Chemother*. 59, 344-55 **(2015)**

22   W. He, X. Guo, L. Xiao, and M. Feng, Study on the mechanisms of chitosan and its derivatives used as transdermal penetration enhancers. *Int J Pharm*. 382, 234-43 **(2009)**

23   R. Olekhnovitch, B. Ryffel, A. J. Muller, and P. Bousso, Collective nitric oxide production provides tissue-wide immunity during Leishmania infection. *J Clin Invest*. 124, 1711-22 **(2014)**

24   C. Lonez, M. Vandenbranden, and J. M. Ruysschaert, Cationic lipids activate intracellular signaling pathways. *Adv Drug Deliv Rev*. 64, 1749-58 **(2012)**

25   S. Asthana, A. K. Jaiswal, P. K. Gupta, V. K. Pawar, A. Dube, and M. K. Chourasia, Immunoadjuvant chemotherapy of visceral leishmaniasis in hamsters using amphotericin B-encapsulated nanoemulsion template-based chitosan nanocapsules. *Antimicrob Agents Chemother*. 57, 1714-22 **(2013)**

26   H. P. Tzeng, F. M. Ho, K. F. Chao, M. L. Kuo, S. Y. Lin-Shiau, and S. H. Liu, beta-Lapachone reduces endotoxin-induced macrophage activation and lung edema and mortality. *Am J Respir Crit Care Med*. 168, 85-91 **(2003)**

27   U. Gonzalez, M. Pinart, L. Reveiz, and J. Alvar, Interventions for Old World cutaneous leishmaniasis. *Cochrane Database Syst Rev*. CD005067 **(2008)**

28   S. Buates, and G. Matlashewski, Treatment of experimental leishmaniasis with the immunomodulators imiquimod and S-28463: efficacy and mode of action. *J Infect Dis*. 179, 1485-94 **(1999)**

29   J. El-On, E. Bazarsky, and R. Sneir, Leishmania major: in vitro and in vivo anti-leishmanial activity of paromomycin ointment (Leshcutan) combined with the immunomodulator Imiquimod. *Exp Parasitol*. 116, 156-62 **(2007)**

30   P. Saha, D. Mukhopadhyay, and M. Chatterjee, Immunomodulation by chemotherapeutic agents against Leishmaniasis. *Int Immunopharmacol*. 11, 1668-79 **(2011)**

31   P. M. Daftarian, G. W. Stone, L. Kovalski, M. Kumar, A. Vosoughi, M. Urbieta, P. Blackwelder, E. Dikici, P. Serafini, S. Duffort, R. Boodoo, A. Rodriguez-Cortes, V. Lemmon, S. Deo, J. Alberola, V. L. Perez, S. Daunert, and A. L. Ager, A targeted and adjuvanted nanocarrier lowers the effective dose of

liposomal amphotericin B and enhances adaptive immunity in murine cutaneous leishmaniasis. *J Infect Dis*. 208, 1914-22 **(2013)**

32   P. Saha, S. Bhattacharjee, A. Sarkar, A. Manna, S. Majumder, and M. Chatterjee, Berberine chloride mediates its anti-leishmanial activity via differential regulation of the mitogen activated protein kinase pathway in macrophages. *PLoS One*. 6, e18467 **(2011)**

33   A. Ukil, A. Biswas, T. Das, and P. K. Das, 18 Beta-glycyrrhetinic acid triggers curative Th1 response and nitric oxide up-regulation in experimental visceral leishmaniasis associated with the activation of NF-kappa B. *J Immunol*. 175, 1161-9 **(2005)**

34   D. Lee, J. Bae, Y. K. Kim, M. Gil, J. Y. Lee, C. S. Park, and K. J. Lee, Inhibitory effects of berberine on lipopolysaccharide-induced inducible nitric oxide synthase and the high-mobility group box 1 release in macrophages. *Biochem Biophys Res Commun*. 431, 506-11 **(2013)**

35   T. Uto, O. Morinaga, H. Tanaka, and Y. Shoyama, Analysis of the synergistic effect of glycyrrhizin and other constituents in licorice extract on lipopolysaccharide-induced nitric oxide production using knock-out extract. *Biochem Biophys Res Commun*. 417, 473-8 **(2012)**

36   T. Dai, M. Tanaka, Y.-Y. Huang, and M. R. Hamblin, Chitosan preparations for wounds and burns: antimicrobial and wound-healing effects. *Expert Review of Anti-Infective Therapy*. 9, 857-879 **(2011)**

37   G. Peluso, O. Petillo, M. Ranieri, M. Santin, L. Ambrosio, D. Calabro, B. Avallone, and G. Balsamo, Chitosan-mediated stimulation of macrophage function. *Biomaterials*. 15, 1215-20 **(1994)**

38   G. I. Howling, P. W. Dettmar, P. A. Goddard, F. C. Hampson, M. Dornish, and E. J. Wood, The effect of chitin and chitosan on the proliferation of human skin fibroblasts and keratinocytes in vitro. *Biomaterials*. 22, 2959-66 **(2001)**

39   S. Nylen, and L. Eidsmo, Tissue damage and immunity in cutaneous leishmaniasis. *Parasite Immunol*. 34, 551-61 **(2012)**

40   D. O. Moon, Y. H. Choi, N. D. Kim, Y. M. Park, and G. Y. Kim, Anti-inflammatory effects of beta-lapachone in lipopolysaccharide-stimulated BV2 microglia. *Int Immunopharmacol*. 7, 506-14 **(2007)**

41   L. Feldmeyer, S. Werner, L. E. French, and H. D. Beer, Interleukin-1, inflammasomes and the skin. *Eur J Cell Biol*. 89, 638-44 **(2010)**

42   G. Meng, F. Zhang, I. Fuss, A. Kitani, and W. Strober, A mutation in the Nlrp3 gene causing inflammasome hyperactivation potentiates Th17 cell-dominant immune responses. *Immunity*. 30, 860-74 **(2009)**

43   S. E. Headland, and L. V. Norling, The resolution of inflammation: Principles and challenges. *Semin Immunol*. **(2015)**

44   K. Kawahara, H. Hohjoh, T. Inazumi, S. Tsuchiya, and Y. Sugimoto, Prostaglandin E-induced inflammation: Relevance of prostaglandin E receptors. *Biochim Biophys Acta*. 1851, 414-421 **(2015)**

45   D. S. Lima-Junior, D. L. Costa, V. Carregaro, L. D. Cunha, A. L. Silva, T. W. Mineo, F. R. Gutierrez, M. Bellio, K. R. Bortoluci, R. A. Flavell, M. T. Bozza, J. S. Silva, and D. S. Zamboni, Inflammasome-derived IL-1beta production induces nitric oxide-mediated resistance to Leishmania. *Nat Med*. 19, 909-15 **(2013)**

46   K. Kautz-Neu, S. L. Kostka, S. Dinges, Y. Iwakura, M. C. Udey, and E. von Stebut, IL-1 signalling is dispensable for protective immunity in Leishmania-resistant mice. *Exp Dermatol*. 20, 76-8 **(2011)**

47   P. Gurung, R. Karki, P. Vogel, M. Watanabe, M. Bix, M. Lamkanfi, and T. D. Kanneganti, An NLRP3 inflammasome-triggered Th2-biased adaptive immune response promotes leishmaniasis. *J Clin Invest*. 125, 1329-38 **(2015)**

48   J. M. Ehrchen, K. Roebrock, D. Foell, N. Nippe, E. von Stebut, J. M. Weiss, N. A. Munck, D. Viemann, G. Varga, C. Muller-Tidow, H. J. Schuberth, J. Roth, and C. Sunderkotter, Keratinocytes determine Th1 immunity during early experimental leishmaniasis. *PLoS Pathog*. 6, e1000871 **(2010)**

49   A. P. Araujo, and S. Giorgio, Immunohistochemical evidence of stress and inflammatory markers in mouse models of cutaneous leishmaniosis. *Arch Dermatol Res*. **(2015)**

50   S. Bhattacharjee, A. Bhattacharjee, S. Majumder, S. B. Majumdar, and S. Majumdar, Glycyrrhizic acid suppresses Cox-2-mediated anti-inflammatory responses during Leishmania donovani infection. *J Antimicrob Chemother*. 67, 1905-14 **(2012)**

51   F. L. Ribeiro-Gomes, and D. Sacks, The influence of early neutrophil-Leishmania interactions on the host immune response to infection. *Front Cell Infect Microbiol*. 2, 59 **(2012)**

52   F. L. Ribeiro-Gomes, A. C. Otero, N. A. Gomes, M. C. Moniz-De-Souza, L. Cysne-Finkelstein, A. C. Arnholdt, V. L. Calich, S. G. Coutinho, M. F. Lopes, and G. A. DosReis, Macrophage interactions with neutrophils regulate Leishmania major infection. *J Immunol*. 172, 4454-62 **(2004)**

Figure Legends

Figure 1. Permeation and penetration studies in pig ear skin for the different formulations and percentage of β-LP quantified in the different skin layers and receptor compartment (RC). Pig ear skin was intact (A), partially damaged (without SC) by tape stripped (B) or highly damaged (tissue without epidermis or dermal membranes, DM) (C). Results are expressed as mean ± SD for at least three independent experiments.

Figure 2. *In vitro* efficacy studies and NO measurement. Anti-amastigote activity in mouse peritoneal macrophages after 48 hours β-LP and β-LP NP treatment without (A) and with imiquimod (IMQ) (B); or unloaded NP without and with IMQ (C). The concentration of DDAB in β-LP NP is four-fold higher than the concentration of β-LP. AmB was used as positive control of infection. After 1 μM AmB treatment, 3.3 ± 1.2 amastigotes per 100 macrophages were found. Nitrite production by infected mouse peritoneal macrophages after 48 hours of treatment with β-LP and β-LP NP without (D) and with IMQ (E); or unloaded NP without and with IMQ (F). The concentration of DDAB in β-LP NP is four-fold higher than the concentration of β-LP. Macrophages stimulated with *E. Coli* LPS (0.1 μg/mL) were used as positive control. Results are expressed as mean ± SD (n=3). Data were analysed using a Mann–Whitney test. * $p < 0.05$; ** $p < 0.01$.

Figure 3. *In vivo* efficacy studies. Lesion size in *L. major* infected BALB/c mice after 21 days of treatment with topical β-LP loaded NP (20 mg/kg daily) or the equivalent of unloaded NP. Results are expressed as median (n=10-12, per group). Multiple comparison between groups were made with a one–way analysis of variance (ANOVA) followed by Dunnet post-test. *** $p < 0.001$ (A). Photograph showing a control mouse (left) and a mouse treated with β-LP NP (right) (B). Parasite burden comparison after 21 days treatment in skin (C), liver (D), spleen (E) and lymph node (F). Results are expressed as median (n=10-12, per group).

Figure 4. Images of skin sections after 21 days of treatment for control (infected untreated mice, A, B, C and D) and mice treated with β-LP NP (E, F, G and H). Sections were stained with H&E (A and E)

and with antibodies against CD3 (lymphocytes, B and F), NIMP-R14 (neutrophils, C and G) and F4/80 (macrophages, D and H), scale bar = 2 mm. Sections stained with anti-CD3 at a final magnification of 5x (B and F), scale bar = 200 μm. NIMP-R14 (neutrophils), F4/80 (macrophages) and CD3 (lymphocytes) staining was quantified using the percentage area stained in each image by counting the number of pixels staining above a threshold intensity and normalising to the total number of pixels. Results are expressed as mean ± SD for 8 mice per group (I). Data were analysed using a Mann–Whitney test. * $p < 0.05$.

Figure 5. Expression of IL-1β (A) and COX-2 (B) in the draining lymph nodes after 21 days of treatment determined by real-time quantitative PCR. Results are expressed as mean ± SD (n ≥ 4). Data were analysed using a Mann–Whitney test. * $p < 0.05$; ** $p < 0.01$.
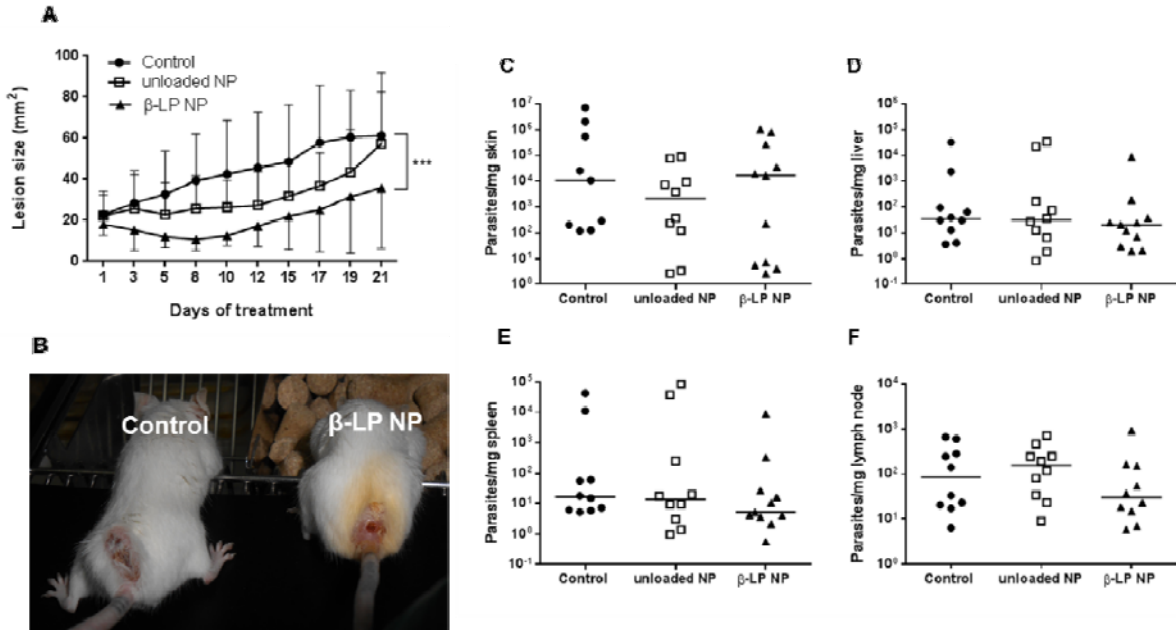
Figure 1
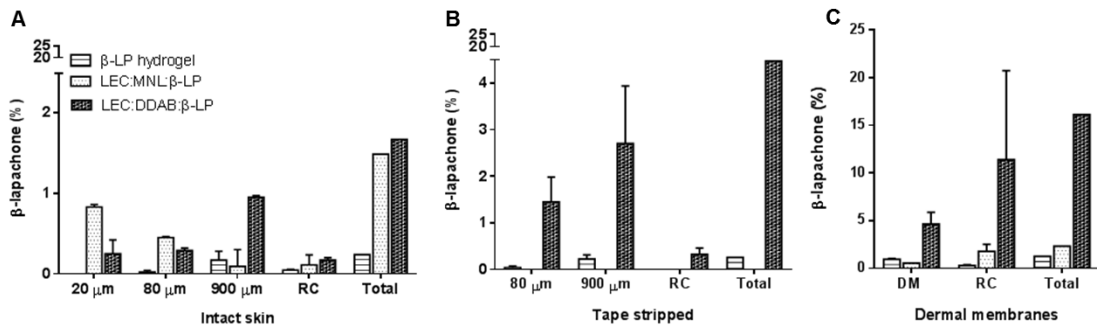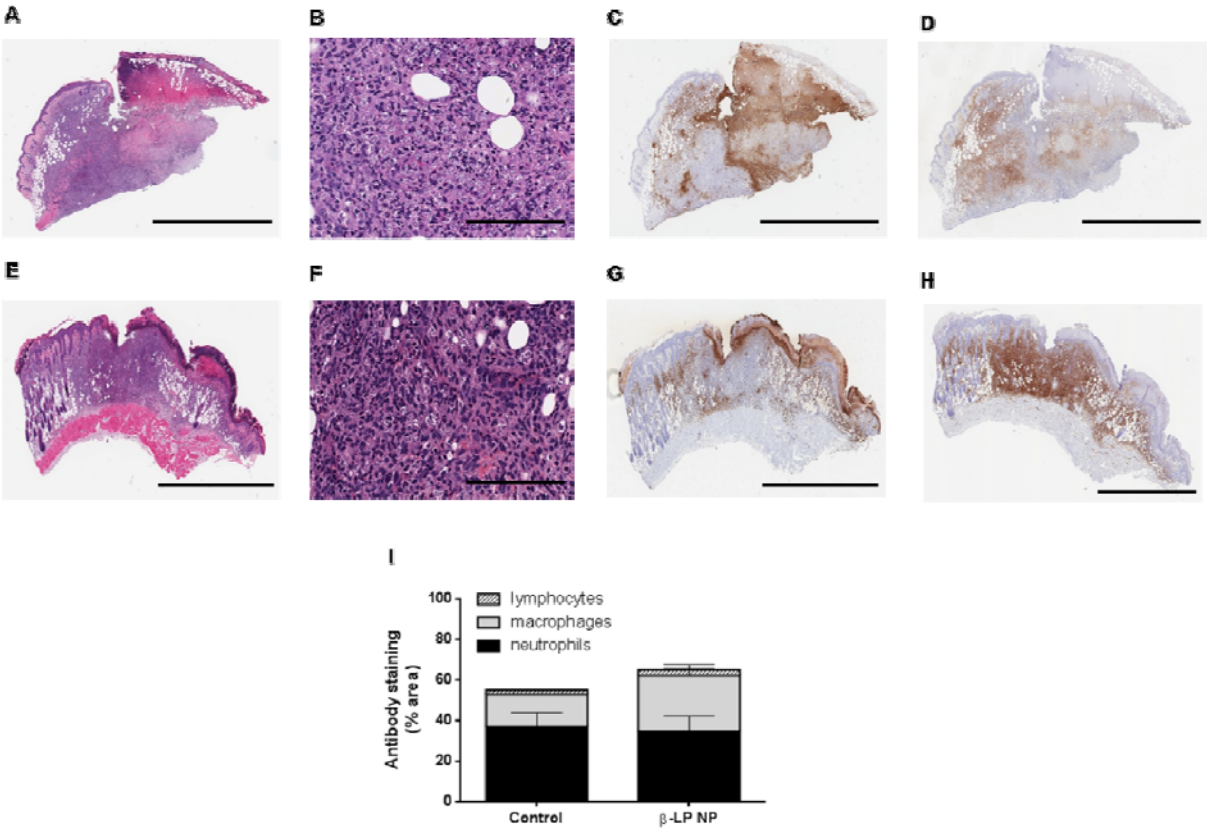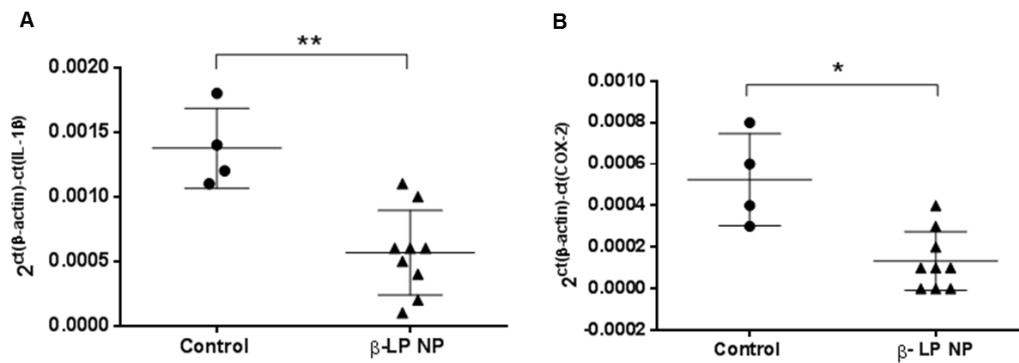

Figure 2
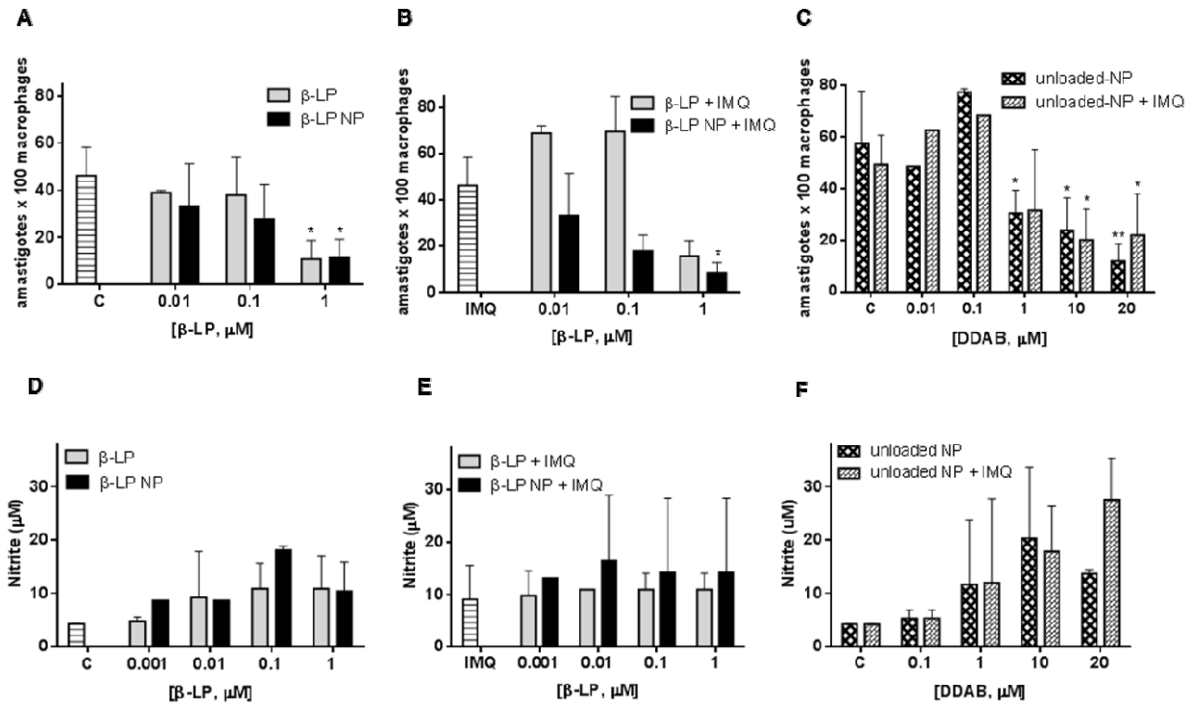
Figure 3

Figure 4

Figure 5

Table 1. Physicochemical properties of unloaded and β-lapachone loaded nanoparticles (NP): diameter, polydispersity index (PI), Z-potential and encapsulation efficiency (EE).

NP composition	Molar ratio (mM)	Diameter (nm)	PI	Z-potential (mV)	EE (%)
LEC*:MNL[†]	75:45	574.2 ± 15.2	0.27	28.5	-
LEC:MNL:β-LP[‡]	75:45:36.5	436.5 ± 6.5	0.27	31.8	25.8 ± 7.4
LEC:DDAB[§]	90:30	317.1 ± 1.9	0.21	88.3	-
LEC:DDAB:β-LP	90:30:36.5	330.1 ± 3.5	0.24	90.2	52.4 ± 2.4

* Lecithin; [†] Monolaurin; [‡] β-lapachone; [§] Didecyldimethylammonium bromide.

Table 2. *In vitro* activity on *Leishmania major* promastigotes and toxicity in mouse peritoneal macrophages for β-lapachone and nanoparticles (NP) after 48 hours of treatment.

NP composition	*L. major* promastigotes IC$_{50}$ (μM)	Peritoneal macrophages IC$_{50}$ (μM)
LEC*:MNL[†] (‡)	80.5 ± 13.5	48.8 ± 2.8
LEC:MNL:β-LP[§] (ǁ)	2.6 ± 0.7	2.1 ± 1.7
LEC:DDAB[¶] (#)	117.7 ± 11.3	34.2 ± 2.1
LEC:DDAB:β-LP (**)	1.9 ± 0.2	3.4 ± 2.1
β-LP	1.5 ± 0.7	6.3 ± 0.6

* Lecithin; [†] Monolaurin; (‡) IC$_{50}$ expressed as [MNL]; [§] β-lapachone; (ǁ) [MNL] =19.2 μM; [¶] Didecyldimethylammonium bromide; (#) IC$_{50}$ expressed as [DDAB]; (**) [DDAB] = 1.4 μM.

Table 3. *In vitro* activity on *Leishmania major* amastigotes and selectivity index (SI) for β-lapachone, unloaded or β-lapachone loaded Lecithin:Didecyldimethylammonium bromide (DDAB) nanoparticles (NP) after 48 hours of treatment.

	L. major amastigotes IC$_{50}$ (µM)	SI
β-LP*	0.7 ± 0.1	9.1
Unloaded NP (†)	3.5 ± 0.8	9.8
β-LP NP (‡)	0.3 ± 0.2	11.3

* β-lapachone; (†) IC$_{50}$ expressed as [DDAB]; (‡) [DDAB] =1.2 µM;

Supplementary Materials

Methods

Chemicals

β-lapachone (3,4-dihidro-2,2-dimetil-2H-nafto[1,2-*b*]piran-5,6-diona, β-LP) was obtained from Tocris Bioscience (Bristol, UK). Emulmetik 930 (95% soybean lecithin, LEC) was kindly gifted by Lucas Meyer Cosmetics (Champlan, France). Chitosan 95/100 (Q 95/100) and chitosan 95/200 (Q 95/200) were supplied by Heppe Medical Chitosan GmbH (Halle, Germany). 2-hydroxipropyl-β-cyclodextrin (HP-β-CD), β-glycerolphosphate (β-GP), 1-monolaurin (1-lauroyl-glycerol, MNL), didecyldimethylammonium bromide (DDAB), sodium hydroxide, 3-(4,5-dimethylthiazol-2-yl)-2, 5-diphenyl-tetrazolium bromide (MTT) and acetonitrile were obtained from Sigma-Aldrich (St. Louis, MO, Canada). Propylene glycol (PG) was obtained from Acofarma (Barcelona, Spain). Lactic acid was supplied by Sharlau (Barcelona, España). Ethanol absolute and acetone absolute were supplied by Panreac (Barcelona, Spain). All other reagents were of analytical grade and were used without further purification.

Cell culture

Mouse peritoneal macrophages isolated from BALB/c mice were cultured in RPMI 1640 medium (Invitrogen, Carlsbad, CA, USA) supplemented with 10% heat-inactivated fetal bovine serum (FBS) (Gibco, Gaithersburg, MD, USA), 100 μg/mL penicillin and 100 μg/mL of streptomycin solution (Sigma, St Louis, MO, USA) in 5% CO_2 at 37 °C. 3T3 mouse fibroflast cell line was cultured in Dulbecco´s modified Eagle´s medium (DMEM, Gibco) containing 10% FBS, 2 mM L-glutamine (Gibco) and 100 μg/mL each of penicillin/streptomycin (Gibco) in 5% CO_2 at 37 °C.

Parasites

Leishmania major promastigotes (clone VI, MHOM/IL/80/Friendlin) were maintained at 26 °C in continuos stirred Schneider´s modified medium (Sigma) supplemented with 10% FBS and 40 mg/ml of gentamicin (Sigma) in flasks. Procyclics were obtained after 1-2 days culture and metacyclics were selected from 5 to 6 days stationary cultures by treatment with peanut agglutinin (PNA) (Sigma). Briefly, stationary promastigote cultures were washed twice in phosphate buffered saline (PBS, pH=7.4, Gibco), resuspended to 2 mL of RPMI 1640 medium and incubated with 20 μg/mL of PNA (5

mg/mL in PBS) to select *L. major* metacyclics. After 20 minutes of incubation, 10 mL of RPMI 1640 were added carefully and the suspension was centrifuged (Allegra X-30 centrifuge, Beckman Coulter, Fullerton, CA, USA) at 500 rpm for 5 minutes. The non-agglutinated promastigotes were collected, washed two times in PBS and used throughout the work.

Animals

BALB/c mice (Harlan, Spain) weighing approximately 20 g and 8 weeks of age were kept under conventional conditions with free access to food and water. Animals were housed in groups of 5 in plastic cages in controlled environmental conditions (12:12 hours light/dark cycle and 22 ± 2 °C). This study was conducted according to ethical standards approved by the Animal Ethics Committee of the University of Navarra in strict accordance with the European legislation in animal experiments.

Preparation and characterization of β-lapachone nanoparticles

β-LP NP were prepared following the procedure reported by Sonvico et al. with modifications [18]. Briefly, different stock solutions of LEC (600 mg/mL), DDAB (50 mg/mL) and MNL (100 mg/mL) were dissolved in ethanol absolute and filtered (0.22 µm). Chitosan (Q 95/100) was solubilised 2% (w/v) of lactic acid at 1% (w/v) concentration and β-LP (10 mg/mL) was also dissolved in the ethanolic solution of LEC. The organic phase was prepared by mixing LEC:DDAB solutions (60:30 mM, respectively) or LEC:MNL solutions (75:45 mM, respectively) with acetone absolute in a 5:4 ratio, respectively. Immediately afterwards, β-LP NP suspensions were obtained by injection of 4 mL of this organic mixture (syringe inner diameter 0.75 mm) into 4 mL of the chitosan aqueous solution magnetically stirred (800 rpm). Then, the organic solvents were evaporated in a rotavapor (Buchi R-144, Flawil, Switzerland) at 40 °C and non-entrapped β-LP was separated from β-LP-loaded NP by centrifugation at 3,000 rpm for 5 minutes (Hettich Mikro 220R, Tuttlingen, Germany). The supernatant, which contained β-LP NP, was recovered for further characterization and the pellet was discarded. Moreover, unloaded NP were prepared for comparison under the same protocol.

The particle size distribution and zeta potential of the NP were measured by photon correlation spectroscopy (PCS) and electrophoretic laser Doppler anemometry, respectively, using a Zetaplus apparatus (Brookhaven Instrument Corporation, USA). The diameter of the NP was determined after dispersion in distilled water (1:10) and measured at 25 °C with a scattering angle of 90 °C. The zeta

potential was measured after dispersion of the NP in 1 mM pH 6 KCl solution. Formulations were placed in glass vials, stored in the dark at 4 °C and kept no more than 1 week.

Determination of β-lapachone loading

The encapsulation efficiency (EE%, amount of β-LP encapsulated/total amount of β-LP x 100) was determined for each batch. Ethanol 70% was added to a known volume of the recovered supernatant containing β-LP NP and sonicated for 1 minute in order to digest the NP. Then, the amount of β-LP was quantified in duplicate by UV-Visible spectrophotometry at 257 nm (Agilent 8453, Waldbronn, Germany). For calculations, calibration curves were designed over the range of 0.5 and 12 µg/mL ($R^2 >$ 0.95).

Preparation of β-lapachone hydrogel

Approximately 1 mL of chitosan hydrogel containing β-LP was prepared according with the following method. Firstly, to solubilise β-LP (10 mg/mL), 100 µl of ethanol absolute were needed. The dissolved drug was mixed with 250 µL of an aqueous HP-β-CD solution. Then, the mixture was added to 250 µL of an aqueous β-GP solution containing 20 µL of PG and, after stirring, it was added to 500 µL of chitosan (Q 95/200), which was previously dissolved in an aqueous solution with lactic acid 2% (w/v). Finally, the mixtures were stirred on a vortex and subsequently loaded on a metal sample plate to allow the gelation process. The final concentrations for β-GP, chitosan (Q 95/200) and HP-β-CD were 30% (w/v), 1% (w/v) and 11.6% (w/v), respectively. All formulations were prepared 24 hours before the study and were stored, protected from light, in glass vials at 4 °C.

Preparation of pig ear skin

Skin cultures were obtained from domestic pig ears in a local slaughterhouse. Ears were taken from the animals and transported to the laboratory in a maximum of 2-3 hours. After washing with tap water, the outer region of the ear was excised with a scalpel and sectioned at a thickness of ca. 1 mm using a dermatome (Aesculap GA 630, Tuttlingen, Germany). Then, skins were stored in Parafilm[®] (Bemis, Neenah, WI, USA) at − 20 °C for no longer than a month. Studies were carried out with intact skin and damaged skin (without stratum corneum or epidermis). Before the experiments, the skin was allowed to thaw at room temperature in PBS for 30 minutes.

In the case of damaged skin, tape stripping procedure was performed. Adhesive tape (Scotch Transparent Tape 600, 3M, St. Paul, MN, USA) was applied pressing onto the skin and then removed

with one quick movement. To determine the number of adhesive applications required to eliminate the stratum corneum (SC), 0, 15, 30 and 60 tapes were applied. After that, samples were staining with Mayer's hemalun (Merck Darmstadt, Germany) and analyzed under a microscope (Olympus BH2, Hamburg, Germany). It was observed that 30 pieces of adhesive tape were necessary to remove all the SC.

In the studies with dermal membranes (without epidermis), full-thickness skin was immersed in water at 60 °C for 45 seconds to separate the epidermal layer.

In vitro permeation studies

Permeation studies using Franz diffusion cells were carried out on a MicroettePlus™ apparatus (Hanson Research Corp., Chatsworth, CA, USA). Transcutaneous diffusion was assessed according to OECD guideline 428. The Franz cell receptor compartments (4 mL) were filled with HP-β-CD 25% (w/v) in PBS to ensure that sink conditions were maintained over the time course of the experiment. Moreover, the receptor medium was homogenised by magnetic stirring (400 rpm) and maintained at 32 ± 1 °C. Skin biopsies were placed horizontally between the donor and the receptor compartments with the SC, epidermis or dermis side up, ensuring their contact with the receptor medium. The whole device was then fixed with a clamp.

All Franz diffusion cell experiments were conducted under infinite doses conditions: 150 μL of the different β-LP formulations (solution, hydrogel and NP) were deposited on 1.74 cm^2 of skin in the donor compartment. The punch areas were devoid of visible structural changes (scratches, erosion or scars) as such skin damage could affect the diffusion and metabolism of the tested compound.

The drug diffusion kinetic was evaluated by automatically sampling 1 mL aliquots of the receptor fluid at the following predetermined times: 0, 0.5, 1, 3, 6, 8 and 24 hours. Each aliquot withdrawn was replaced with an equal volume of receptor phase. Franz cell blank experiments were conducted with the formulations without drug. At the end of the experiment, the excess of formulation was removed and the skin pieces were stored at – 80 °C for some minutes. Then, the skin samples were embedded in OCT compound (Optimal Cutting Temperature compound, Tissue-Tek, Sakura Finetek, Villeneuve d'Ascq, France) and frozen again to make the cuts aesier. Skin sections were cut using a microtome cryostat (Leica CM 1900, Leica Microsystems, Schweiz, AG, Germany) and, after separating the SC (20 μm), the epidermis (80 μm) and the dermis (900 μm), the drug concentration in each layer was determined.

Skin sections were pretreated with trypsin (1.5% (v/v), Gibco) and collagenase D (300 µg/mL, Roche, Basel, Switzerland) in 70% ethanol for 12 hours at 4 °C. Then, skin biopsies were homogenized for 1 minute using an ultrasonic cell disruptor (Misonix, Farmingdale, NY, USA). The amount of β-LP was quantified by HPLC-UV. Analysis was carried out in a 1100 series LC (Agilent, Germany) with a diode-array detector set at 257 nm. The chromatographic system was equipped with a reversed-phase 150 mm x 2.1 mm C18 Alltima column (5 µm particle size; Altech, USA) and a Gemini C18 precolumn (5 µm particle size; Phenomenex, CA, USA). The mobile phase, pumped at 0.25 mL/min, was a mixture of acetonitrile and water (1:1). Under these conditions, β-LP eluted at 5.8 ± 0.2 min. For calculations, calibration curves were designed over the range of 0.5 and 12 µg/mL (R^2> 0.999). Results are expressed as mean ± SD for at least three independent experiments.

In vitro antileishmanial activity against L. major promastigotes

The antileishmanial effect of β-LP, β-LP NP (with DDAB or MNL) or unloaded NP was determined in *L. major* promastigotes by the MTT assay. Briefly, 2 x 10^5 parasites per well were seeded in 96-well plates with different concentrations of β-LP or NP (ranging from 0 to 200 µM). Plates were then incubated at 26 °C for 48 h. Previously, β-LP was disolved in DMSO (Sigma-Aldrich). Untreated cells were used as control and cells treated with Amphotericin B (AmB, Sigma) were used as positive control. After incubation, 20 µL of a MTT solution (5 mg/mL in PBS) were added to each well and plates were incubated at 26 °C for 4 h. To ensure complete solubilisation of the formazan crystals, 50 µL of 10% SDS in 0.01 M HCl lysing buffer was added and plates were gently shaken for 20 minutes. Parasite viability was determined using a microplate reader (iEMS Reader MS, Labsystems) at 570 nm. Results are expressed as mean ± SD for at least three independent experiments in duplicate.

In vitro cytotoxicity assay in mouse peritoneal macrophages

To estimate the toxicity of β-LP, β-LP NP (with DDAB or MNL) or unloaded NP, an *in vitro* cytotoxicity assay was performed in mouse peritoneal macrophages using Alamar Blue (AB). Briefly, BALB/c mice were inoculated with 1 mL of 3% (w/v) thioglycolate (Sigma-Aldrich). After 3 days, animals were euthanized by cervical dislocation and 5 mL of cold RPMI 1640 medium were injected into the peritoneal cavity and then recovered with a syringe. Cells were collected from the peritoneal fluid by centrifugation (Allegra X-30 centrifuge, Beckman Coulter, Fullerton, CA, USA) at 1,500 rpm for 10 minutes. Then, the pellet was resuspended in RPMI 1640 supplemented with 10% FBS, 1% of a 100

U/mL penicillin and 100 μg/mL of streptomycin solution (Sigma). Macrophages were adjusted to 2.5 x 10^4 cells per well and cultured in supplemented RPMI 1640 in 96-well plates at 37 °C under 5% CO_2 for 24 hours. Then, different concentrations of β-LP and NP (0 to 300 μM) were added to wells and plates were incubated again for 48 hours. After 48 hours incubation, 20 μL of the AB reagent solution (final concentration of AB=10% (v/v)) (Invitrogen) were added to wells and plates were incubated for 4 hours. Finally, sample flourescences were measured using a microplate fluorimeter (λ excitation 560 nm; λ emission 590 nm; Polar Star Galaxy, BMG Labtechnologies, Offenburg, Germany). Results are expressed as mean ± SD for at least three independent experiments in duplicate.

Effect of β-lapachone and β-lapachone nanoparticles on L. major amastigotes in vitro

Peritoneal macrophages of BALB/c mice were collected and cultured as described above. Macrophages in a concentration of 5 x 10^4 were seeded in Labtek plates (BD Biosciences, Franklin Lakes, IL, USA) and incubated at 37 °C with humidified atmosphere containing 5% CO_2. After 24 hours incubation, macrophages were washed with RPMI 1640 medium and infected with metacyclic promastigotes of *L. major*, isolated as previously described, in a 7:1 proportion (parasites:macrophages). Infected cells were incubated overnight at 37 °C. Then, wells were washed twice with RPMI 1640 and treated with β-LP, β-LP NP or unloaded NP at different concentrations for 48 hours at 37 °C. The same experiments were also carried out with the addition of 0.1 μg/mL of Imiquimod (IMQ, Sigma-Aldrich) to wells. AmB was used as reference drug and untreated infected cells were used as a positive control of infection. After 48 hours, slides were fixed with methanol and stained with Giemsa for evaluation (Merck Darmstadt, Germany) [19]. The percentage of infected macrophages was evaluated by counting 200 macrophages using an optical microscope (Nikon Eclipse E400 + Y-THM + Y-THR, Chiyoda-ku, Tokyo, Japan). Experiments were performed at least three times in duplicate and results are presented as mean ± SD.

Measurement of nitric oxide

Nitrite (NO^{2-}) accumulation in cell culture supernatants of infected peritoneal macrophages was used as an indicator of nitric oxide (NO) production and it was determined by the Griess reaction. Briefly, 100 μL of culture supernatants from macrophage culture were dispensed in 96-well plates. Then, 100 μL of the Griess reagent (Sigma) were added to each well and plates were incubated at room temperature for 20 minutes. The optical density of the coloured product formed was measured on a

microplate reader (iEMS Reader MS, Labsystems) at 570 nm. The amount of NO formed in each sample was calculated by comparing them with a standard sodium nitrite ($NaNO_2$) concentration curve. 0.1 μg/mL of *Escherichia Coli* lipopolysaccharide (*E. Coli* LPS, Sigma-Aldrich) was use as positive control. Results are expressed as mean ± SD for at least three independent experiments.

Wound healing studies

Firstly, the cytotoxicity of β-LP, β-LP NP or unloaded NP was determined in 3T3 mouse fibroblasts after 24 hours of treatment by the MTT assay, as described in the *in vitro* antileishmanial studies. For the wound healing studies cells were grown to confluence on 6-well plates. Then, cell culture media was gently aspirated and single horizontal scratches were done in the centre of each well with a 200 μL sterile plastic tip. After washing the wells twice with PBS, different concentrations of β-LP, β-LP NP or unloaded NP were suspended in 2 mL of new fresh media and added to each well. Plates were maintained at 37 °C and 5% CO_2. The filling up of the gaps was monitored by taking images (10x) each 15 minutes during 12 hours (10 random fields were examined for each well) using an Zeiss observer Z1 microscope. The wound healing area was determined by computer using the Fiji WH 2.0 software. Results are expressed as percentage of wound healing of three independent experiments (mean ± SD).

Infection

Animals were infected by subcutaneous inoculation of 100 μL of PBS containing 2 x 10^5 infective metacyclic promastigotes (isolated as previously described) of *L. major* in the base of the tail. Lesions were measured each 2 days with a digital caliper.

In vivo evaluation of β-lapachone formulations in L. major-infected BALB/c mice

After 5-7 weeks, lesions of measurable size (average area of 20 mm^2) developed and treatment with 20 mg/kg of β-LP NP or the equivalent of unloaded NP were initiated (10-12 mice per group). Untreated infected mice were used as control. Lesions were covered with 100 μL of the NP formulations (β-LP NP (5 mg/mL) or unloaded NP). Topical treatment was applied daily for a period of 21 days. Once treatments were finished, animals were kept for 3 days before sacrifice. Final results are expressed as mean of the lesion area (mm^2) ± SD measured with a caliper. Moreover, the parasitic load was quantified by a limiting-dilution assay. Firstly, skin fragments from ulcerated lesions as well as spleen, liver and popliteal lymph of infective mice were aseptically removed and treated with

collagenase D in collagenase buffer (10 mM Hepes pH 7.4, 150 mM NaCl, 5 mM KCl, 1 mM MgCl$_2$ and 1.8 mM CaCl$_2$; final collagenase concentration: 2 mg/ml) for 20 minutes at 37 °C. Then, samples were homogenized in 20 mL of RPMI 1640 medium (Gibco) with a sterile syringe piston and centrifuged at 1,250 rpm for 5 minutes for sedimentation (Allegra X-30 centrifuge, Beckman Coulter, Fullerton, CA, USA). The pellet was resuspended in RPMI 1640 medium and 2 mL of lysis buffer (0.14 M ammonium chloride in 17 mM Tris-HCl) were added. After 2 minutes at 37 °C, 20 mL of RPMI 1640 were added and samples were centrifuged at 1,250 rpm for 5 minutes. The pellet was resuspended in 1 mL of Schneider´s modified medium supplemented with 10% heat-inactivated FBS and 40 µg/ml of gentamicin (Sigma, St. Louis, MO, Canada). The homogenate was submitted to serial dilutions in triplicates in sterile 96 well culture plates and incubated at 26 °C. Each well was examined for the presence of parasites and the number of parasites was quantified by the highest dilution at which parasites could grow over a 7-10 day period. The lowest dilution at which parasites were detected was 10^{-1}, which was considered the limit of quantification. Results are expressed as the median calculated per group.

Histological analysis and immunohistochemistry

Skin lesions were formalin-fixed, paraffin-embedded and cut in 3-µm thick sections. Some sections were stained with hematoxylin and eosin (HE) and Masson trichrome. In addition, immunohistochemistry was applied using the following primary antibodies: rat anti-mouse F4/80 (1:400; eBiosciences, 14-4801), rat anti-mouse NIMP-R14 (1:10000; Abcam, ab2557), rabbit anti-CD3 (1:300; Thermo Scientific, RM9106) and rabbit anti-iNOS (1:500; Santa Cruz Biotechnology, sc-650). Antigen retrieval was applied: 2 µg/ml proteinase K at 37 °C for 30 minutes (for F4/80 and NIMP-R14) or heating for 30 minutes at 95 °C in 0,01 M Tris-1 mM EDTA pH 9 in a Pascal pressure chamber (Dako, S2800) (for CD3 and iNOS). In the case of rat primary antibodies, sections were first incubated with rabbit anti-rat (Dako, E0468) secondary antibody. Then, the EnVision system (Dako, K4011) was used in all cases according to manufacturer instructions. For each assay, digital images were scanned using a digital microscope system (Aperio ScanScope CS2, Leica Biosystems, Nussloch, Germany) and snapshots of higher magnification images were captured using image software (Aperio ImageScope, Leica Biosystems). Then, the percentage area stained in each image was then quantified by counting the number of pixels staining above a threshold intensity and normalising to the

total number of pixels. Threshold intensity was set such that only clearly stained pixels were counted. The software used was Fiji WH 2.0.

RNA extraction and quantitative real time RT-PCR

Before RNA extraction, lymph nodes were homogenized in 1 mL of Tri Reagent (Sigma-Aldrich) and total RNA was obtained following the Tri Reagent protocol. Total RNA (1 µg) was treated with DNase (Gibco-BRL) prior to RT with M-MLV reverse transcriptase (Gibco-BRL) in the presence of RNaseOUT (Gibco-BRL). IL-1β, Cox-2, iNOS, IL-4, TNF-α, IFN-Y, TGF-β and β-actin expression were measured by quantitative real time PCR using iQ SYBR Green supermix (Bio-Rad) and specific primers for each gene (see Supplementary Table 1) in a CFX96 system from Bio-Rad. The amount of each transcript was expressed by the formula: 2ct(β-actin)−ct(gene), being ct the point at which the fluorescence rises appreciably above the background fluorescence.

Statistical Analysis

Statistical significance was analyzed using Prism 6.0 software (Graphpad Software Inc., San Diego, CA, USA). Differences were tested using the Mann–Whitney test for two groups comparison or the One–Way ANOVA with Dunn´s post-test for multiple comparison (*in vivo* study of efficacy). * $p < 0.05$; ** $p < 0.01$; *** $p < 0.001$.
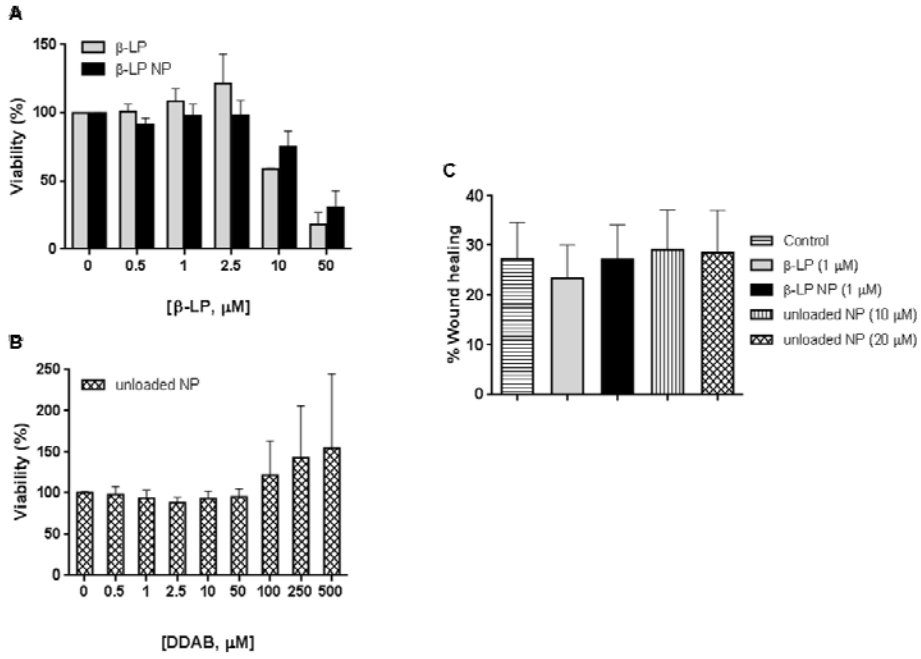
Supplementary Tables

Supplementary Table 1. Primers used in this study.

Gene	Sense primer (5´-3´)	Antisense primer (5´-3´)
Cox-2	CAAAAGCTGGGAAGCCTTCTC	CCTCGCTTATGATCTGTCTTG
IL-1β	GCCACCTTTTGACAGTGATG	TAATGGGAACGTCACACACC
iNOS	TCCTACACCACACCAAACTG	AATCTCTGCCTATCCGTCTC
IL-4	GCTATTGATGGGTCTCAACC	TCTGTGGTGTTCTTGTTGC
TNF-α	CTTCCAGAACTCCAGGCGGT	GGTTTGCTACGACGTGGG
IFN-Y	TCAAGTGGCATAGATGTGGAAGAA	TGGCTCTGCAGGATTTTCATG
TGF-β	CGGCAGCTGTACATTGAC	TCAGCTGCACTTGCAGGAGC
β-actin	CGCGTCCACCCGCGAG	CCTGGTGCCTAGGGCG

Supplementary Figures

Supplementary Figure 1

Supplementary Figure 2
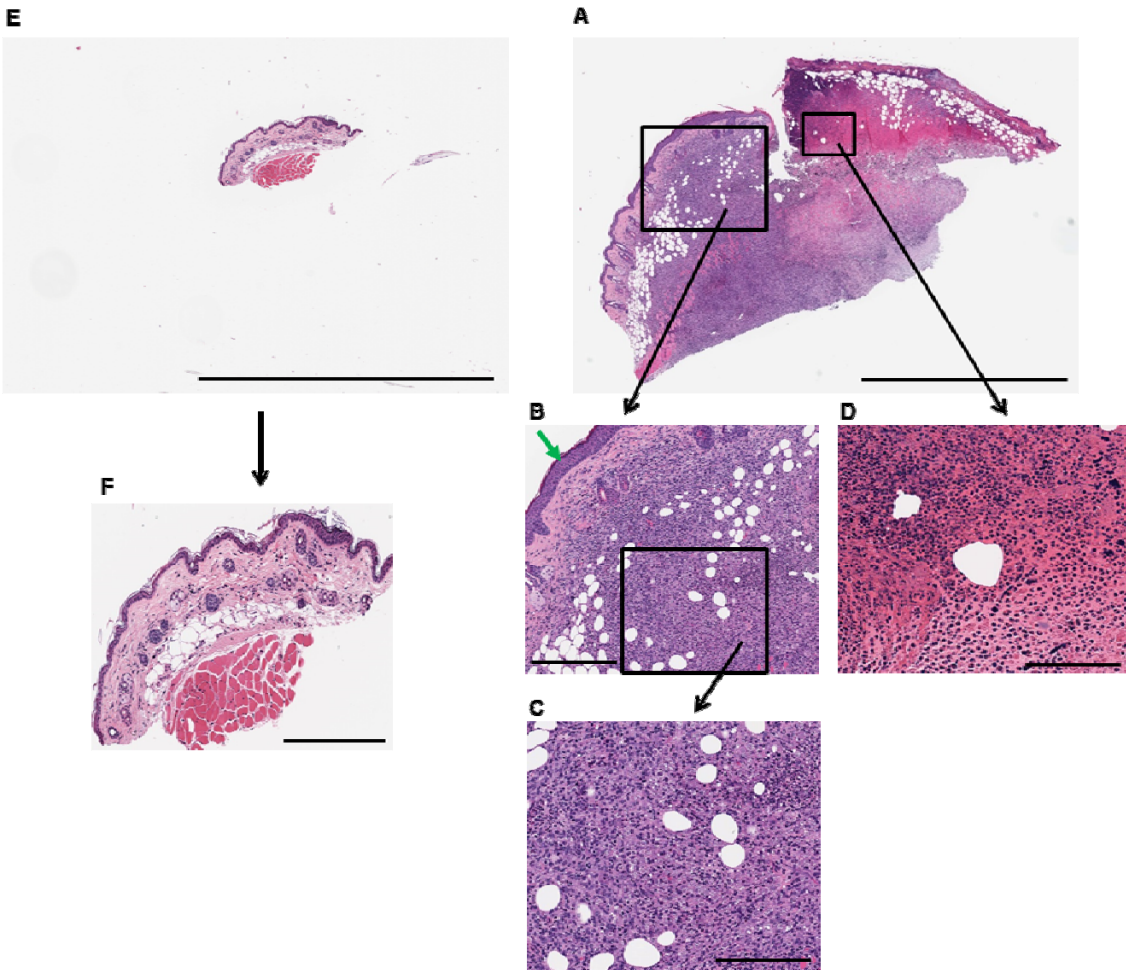
Supplementary Figure Legends

Supplementary Figure 1. Proliferative and wound healing studies. Percentage of 3T3 fibroblasts viability after 24 hours treatment with β-LP and β-LP NP (A) or unloaded NP (B). Percentage of wound healing in 3T3 fibroblasts treated with β-LP, β-LP NP or unloaded NP after 12 hours (C). The concentration of DDAB in β-LP NP is four-fold higher than the concentration of β-LP. Results are expressed as mean ± SD (n=3).

Supplementary Figure 2. H&E stained skin sections obtained for a control mouse (infected and non-treated, A, B, C and D) and healthy mouse (non-infected and non-treated, E and F). (A) Scanned CL lesion shows two clear areas: an inflamed region (magnified in B and C), and the necrotic tissue (magnified in D), scale bar = 2 mm. (B) Inflamed area with epidermal hyperplasia (green arrow) and impressive infiltration of infected macrophages and free parasites (magnified in C) that disturb the subcutaneous and muscular layers, final magnification of 10x, scale bar = 300 μm. (C) Detail of infected macrophages and parasites, final magnification of 20x, scale bar = 200 μm. (D) Detail of necrotic and granulation tissue, final magnification of 20x, scale bar = 200 μm. (E, F) Scanned healthy skin to clearly appreciate the hyperkeratosis and inflammation, E, scale bar = 2 mm and F, final magnification of 10x, scale bar = 300 μm.